

Anisotropic superconducting energy gap in Pb[†]

P. G. Tomlinson and J. P. Carbotte

Physics Department, McMaster University, Hamilton, Ontario L8S 4M1, Canada

(Received 9 June 1975)

We have calculated directional electron-phonon effective distribution functions $\alpha_{\vec{k}}^2(\omega)F_{\vec{k}}(\omega)$ at many points on the Pb Fermi surface. From these distributions the zero-temperature energy gaps in superconducting Pb single crystals follow from one iteration of the directional Eliashberg equations. Anisotropic mass renormalization parameters are also determined. In the calculations, the Pb Fermi surface is obtained from a four-plane-wave model pseudopotential chosen to fit the de Haas-van Alphen data. The four-plane-wave electron states are used in evaluating the electron-phonon interaction which in addition depends on the lattice dynamics. This is taken from experiments on the dispersion curves for the phonons.

I. INTRODUCTION

Measurements of gap anisotropy in pure single-crystal Pb have been reported by Blackford,¹ who uses the technique of superconducting tunneling into a pure oriented single crystal. Experiments also exist in which the anisotropy in thick Pb films²⁻⁴ is investigated. More often, however, "dirty" thin films have been investigated in which the anisotropy is ignored.⁵ Such dirty films of Pb are the classic example of a strong-coupling superconductor, and the Eliashberg gap equations have been applied to describe them with remarkable success. In their usual dirty-limit form, the anisotropy has been assumed to be washed out and the basic equations refer only to a frequency-dependent gap parameter which does not vary with position on the Fermi surface. In this case it has been possible to invert the Eliashberg equations to obtain detailed information on the interactions involved in superconductivity. Tunneling data on the current (I)-voltage (V) characteristics of a tunnel diode can be used as input from which we can derive a function $\alpha^2(\omega)F(\omega)$ referring to the electron-phonon interaction and a parameter U_C related to the basic Coulomb repulsions between electrons. It is in fact these two quantities that make up the kernels of the Eliashberg equations. They contain within them all the information on the electronic structure and the lattice dynamics as well as the electron-phonon interaction that is required to calculate the superconductivity properties of a given material.

For an anisotropic, single-crystal superconductor, more complex equations which refer to new frequency- and momentum-dependent gap parameters are needed. It is out of the question, at the moment, to iterate these four-dimensional equations. Because of this, Bennett⁶ has suggested that we make a single iteration of these equations based on the dirty-limit solutions of the one-dimensional Eliashberg equations. While this involves an approximation, it does give tractable expressions.

The kernels entering the directional Eliashberg equations are U_C , as before, and directional electron-phonon functions $\alpha_{\vec{k}}^2(\omega)F_{\vec{k}}(\omega)$. One such function is needed for each electron state $|\vec{k}\rangle$ on the Fermi surface. The Fermi-surface average of $\alpha_{\vec{k}}^2(\omega)F_{\vec{k}}(\omega)$ is simply the isotropic function $\alpha^2(\omega) \times F(\omega)$ which is measured in thin-film tunneling experiments. More specifically,

$$\alpha^2(\omega)F(\omega) = \left(\int \frac{dS_{\vec{k}}}{\hbar|\vec{V}(\vec{k})|} \alpha_{\vec{k}}^2(\omega)F_{\vec{k}}(\omega) \right) / \int \frac{dS_{\vec{k}}}{\hbar|\vec{V}(\vec{k})|},$$

where the integral $dS_{\vec{k}}$ is over the Fermi surface $\vec{V}(\vec{k})$ is the Fermi velocity associated with the state $|\vec{k}\rangle$, and \hbar is Planck's constant over 2π .

To summarize, it is the directional four-dimensional Eliashberg equations that are needed to describe gap anisotropy in superconducting Pb. The kernels in these equations which refer to the normal-state parameters of the system are U_C and $\alpha_{\vec{k}}^2(\omega)F_{\vec{k}}(\omega)$. In a rough way this function can be thought of as a directional phonon frequency distribution in which only those phonons that can scatter the electron $|\vec{k}\rangle$ are included and in which each phonon mode is weighted by the appropriate strength of the electron-phonon interaction. It is these functions that are basic to a microscopic calculation of gap anisotropy in Pb.

The paper is structured as follows: In Sec. II the formula for $\alpha_{\vec{k}}^2(\omega)F_{\vec{k}}(\omega)$ is specified. It is shown to depend on an integral over the Fermi surface of the square of the electron-phonon vertex times a phonon δ function. For the Fermi surface we use a four-plane-wave pseudopotential model adjusted to give a reasonable fit to the de Haas-van Alphen data. The electron-phonon matrix element is needed only for initial and final states, both on the Fermi surface, and is evaluated between four-plane-wave functions with pseudopotential form factors taken from the work of Appapillai and Williams.⁷ The electron-phonon matrix element also depends on the lattice dynamics. This is derived

from a Born-von Kármán force-constant model fitted by Cowley⁸ to all the measured phonon modes in the high-symmetry directions as well as at some off-symmetry points. For this information the $\alpha_{\vec{k}}^2(\omega)F_{\vec{k}}(\omega)$ are calculated at many points on the Pb Fermi surface.

In Sec. III we give results for the average function $\alpha^2(\omega)F(\omega)$, which we calculate and compare with tunneling results on this function. A discussion of the present state of agreement is included. We also compare our results for $\alpha^2(\omega)$ with tunneling-derived experimental values⁵ on its frequency

$$\alpha^2(\omega)F(\omega) = \int \frac{dS_{\vec{k}}}{\hbar|\vec{V}(\vec{k})|} \int \frac{dS_{\vec{k}'}}{\hbar|\vec{V}(\vec{k}')|} \sum_{\lambda} |g_{\vec{k}'\vec{k}\lambda}|^2 \delta(\omega - \omega_{\lambda}(\vec{k}' - \vec{k})) / (2\pi)^3 \int \frac{dS_{\vec{k}}}{\hbar|\vec{V}(\vec{k})|}. \quad (1)$$

All the integrals in Eq. (1) are surface integrals on the Pb Fermi surface, and $dS_{\vec{k}}$ is a surface element. At the point $|\vec{k}\rangle$, the Fermi velocity is denoted by $\vec{V}(\vec{k})$, and $g_{\vec{k}'\vec{k}\lambda}$ denotes the electron-phonon vertex owing to the interaction with a phonon of frequency $\omega_{\lambda}(\vec{k}' - \vec{k})$ with λ a branch index for electron scattering from $|\vec{k}\rangle$ to $|\vec{k}'\rangle$, both states being on the Fermi surface (FS). The δ function on phonon frequencies places the various modes in bins according to the absolute value of $\omega_{\lambda}(\vec{k}' - \vec{k})$.

To calculate the anisotropic energy gap at zero temperature in a pure single crystal of Pb, we will require the functions $\alpha_{\vec{k}}^2(\omega)F_{\vec{k}}(\omega)$ which are obtained from Eq. (1) by dropping the FS average over $|\vec{k}\rangle$. That is,

$$\alpha_{\vec{k}}^2(\omega)F_{\vec{k}}(\omega) = \frac{1}{(2\pi)^3} \int \frac{dS_{\vec{k}'}}{\hbar|\vec{V}(\vec{k}')|}$$

$$g_{\vec{k}'\vec{k}\lambda} = -i \left(\frac{\hbar\Omega}{2MN\omega_{\lambda}(\vec{k}' - \vec{k})} \right)^{1/2} \vec{\epsilon}_{\lambda}(\vec{k}' - \vec{k}) \cdot \left(\sum_{\vec{k}_n} \sum_{\vec{k}_n'} \alpha_{\vec{k}_n}^*(\vec{k}') \alpha_{\vec{k}_n}(\vec{k}) (\vec{k}' + \vec{k}_n' - \vec{k} - \vec{k}_n) \langle \vec{k}' + \vec{k}_n' | W | \vec{k} + \vec{k}_n \rangle \right), \quad (4)$$

with M the ion mass and N the total number of atoms in the crystal. In Eq. (4) $\langle p' | W | p \rangle$ denotes the electron-ion pseudopotential form factor for scattering from the plane-wave momentum \vec{p}' . If we assume a local approximation is adequate, it becomes a function of $\vec{p}' - \vec{p}$ only and is denoted by $W(\vec{p}' - \vec{p})$. The expressions (1) and (2) are now completely specified.

The evaluation of Eqs. (1) and (2) proceeds as follows: The four-plane-wave pseudopotential model⁹ without spin-orbit coupling is used to generate the real Pb Fermi surface. We find that $V_{111} = -0.096$ Ry, $V_{200} = 0.039$ Ry, and $E_F = 0.718$ Ry produces the best fit and is consistent with the Appapillai and Williams⁷ pseudopotential. In Fig.

dependence. Section IV contains a discussion of the isotropic Eliashberg equation as well as the directional one-iteration theory of Bennett.⁶ Finally, in Sec. V we give results for the variation of the gap edge $\Delta_0(\vec{k})$ as a function of $|\vec{k}\rangle$ on the Fermi surface. The mean square anisotropy in $\Delta_0(\vec{k})$ is also evaluated and a short discussion is included.

II. ELECTRON-PHONON FUNCTIONS $\alpha_{\vec{k}}^2(\omega)F_{\vec{k}}(\omega)$

The isotropic electron-phonon function $\alpha^2(\omega)F(\omega)$ which plays the central role in the strong-coupling theory of a dirty superconductor can be written

$$\times \sum_{\lambda} |g_{\vec{k}'\vec{k}\lambda}|^2 \delta(\omega - \omega_{\lambda}(\vec{k}' - \vec{k})). \quad (2)$$

These are central to the work here. We now specify in detail the integrand. We denote the electron wave function at $|\vec{k}\rangle$ by $\phi_{\vec{k}}(\vec{x})$ and expand it in terms of plane waves. It can be written

$$\phi_{\vec{k}}(\vec{x}) = \frac{1}{\sqrt{\Omega}} e^{i\vec{k}\cdot\vec{x}} \sum_{\vec{k}_n} a_{\vec{k}_n}(\vec{k}) e^{i\vec{k}_n\cdot\vec{x}}, \quad (3)$$

where Ω is the crystal volume and the \vec{k}_n stand for the reciprocal-lattice vectors. The expansion coefficients $a_{\vec{k}_n}(\vec{k})$ are needed only for states on the FS; for a four-plane-wave theory only four such quantities are required.

If we denote the phonon polarization vector associated with $\omega_{\lambda}(\vec{k})$ by $\vec{\epsilon}_{\lambda}(\vec{k})$ we can write the electron-phonon vertex $g_{\vec{k}'\vec{k}\lambda}$ in the form

1 we show a cross section of this surface which is the [110] section through the point Γ . We note that while the distortions from a sphere are not enormous, they are nevertheless significant. The calculation of this constant-energy surface yields at the same time the surface elements $dS_{\vec{k}}$ at various points on the FS and the Fermi velocities $\vec{V}(\vec{k})$. The mixing coefficients $a_{\vec{k}_n}(\vec{k})$ are also obtained and retained because they are needed in Eq. (4). This completely specifies the electronic structure.

Besides the electron structure, the lattice dynamics for Pb is also needed. We can calculate $\vec{\epsilon}_{\lambda}(\vec{k})$ and $\omega_{\lambda}(\vec{k})$ at any point by diagonalizing the dynamical matrix at that point. The dynamical matrix can be constructed from a knowledge of a

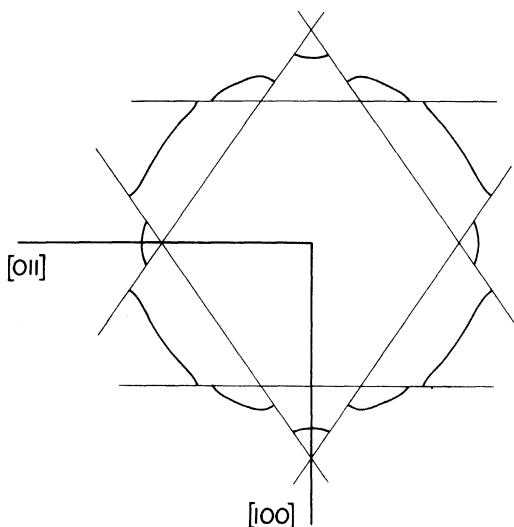


FIG. 1. [110] cross sections through Γ of the Fermi surface of Pb calculated in this work.

Born-von Kármán force-constant system. The choice of Born-von Kármán models requires some care in Pb. The problem is as follows and is worth emphasizing. The phonon dispersion curves for the high-symmetry directions were measured in Pb by Brockhouse *et al.*¹⁰ using inelastic neutron scattering. They also analyze their results in terms of a Born-von Kármán force-constant model. It has been found,¹¹ however, that this model is not reliable for predicting off-symmetry phonons. The reason is that the dispersion curves in Pb are so highly constructed that it is difficult to reproduce off-symmetry phonons from only high-symmetry information. Recently Cowley⁸ has derived a new Born-von Kármán system of force constants by a least-squares fit to the more extensive data of Stedman *et al.*,¹² who sampled phonons throughout the first Brillouin zone (FBZ). It is this new system that we have used in this work. There is some evidence that it is quite reliable. We will want to return to this point shortly.

The final quantity to be specified is the electron pseudopotential form factor $W(\vec{p}' - \vec{p})$. We take it from the recent work of Appapillai and Williams.⁷ This completely specifies $\alpha^2(\omega)F(\omega)$, which can be evaluated on a computer with no approximations. We note that the calculation involves no adjustable parameters. It does rely, however, on the best available data on the Pb Fermi surface as well as on phonon dispersion curves. Also, the pseudopotential of Appapillai and Williams⁷ is a model potential based on the previous work of Shaw¹³ who employs atomic term factor data.

III. RESULTS FOR $\alpha^2(\omega)F(\omega)$

We start with a discussion of our results for the isotropic function $\alpha^2(\omega)F(\omega)$. In Fig. 2 we com-

pare the results of our calculations (solid curve) with the tunneling results obtained by McMillan and Rowell⁵ (dotted curve). We see that the overall agreement is really very good although there is some discrepancy in details. The transverse peak around 4–5 meV is slightly smaller in our calculations than it is in the experiment. It also exhibits somewhat sharper structures. The peak around 9 meV is larger in our work than it is in the tunneling results. It is also sharper and displaced slightly towards higher energies. It also cuts off sharply, while tunneling shows a high-energy tail. These discrepancies, while not large, require some further comments. Before doing this, however, we should stress again that in our calculations the real Pb Fermi surface has been used and the electrons have been treated in a four-plane-wave model. The low-frequency behavior of our curve should therefore be quite reliable, in contrast to the previous one-plane-wave calculations of Carbotte and Dynes¹⁴ which break down in this region.

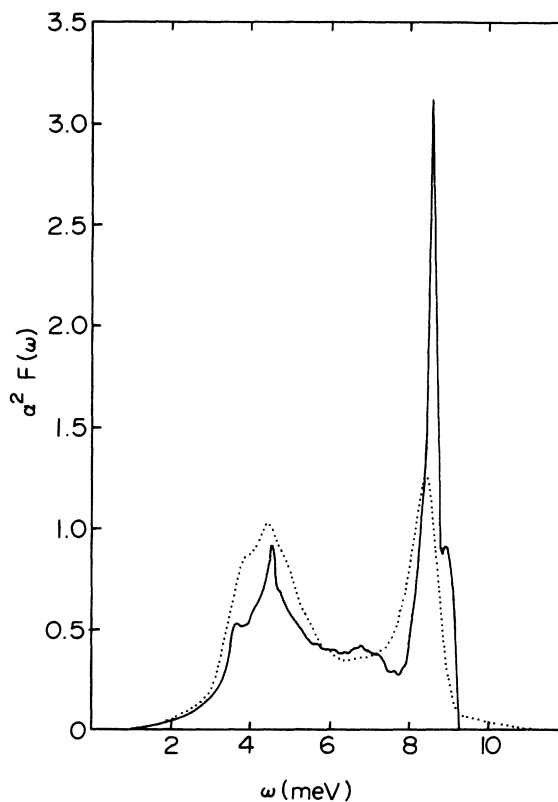


FIG. 2. Comparison of calculated (solid curve) and tunneling-derived (Ref. 5) (dotted curve) isotropic electron-phonon function $\alpha^2(\omega)F(\omega)$ for Pb. Calculations include the real Pb Fermi surface and four-plane waves for the electronic wave functions. For the phonons, the Born-von Kármán model of Cowley was used.

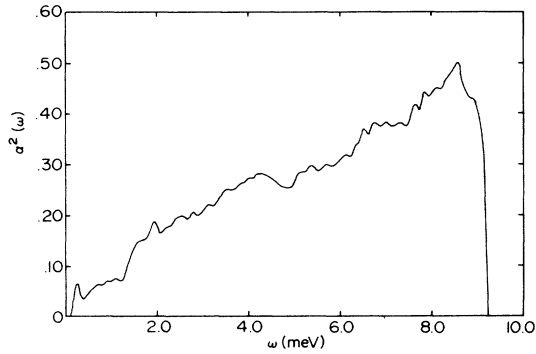


FIG. 3. Square of the isotropic coupling strength $\alpha^2(\omega)$ calculated in this work. We note the sharp increase in $\alpha^2(\omega)$ around 1.6 MeV, which is observed experimentally in Ref. 16.

Recent experiments in the far infrared by Farnworth and Timusk¹⁵ have shown that tunneling does not seem to pick up all the structure that exists in the phonon density of states. These experiments would favor some of the features exhibited in our calculations, although others are still not quite in agreement with experiment. This may indicate some remaining inaccuracy in the force-constant model suggested by Cowley.⁸ Also, if we calculate the mass enhancement parameter λ from our results on $\alpha^2(\omega)F(\omega)$ which is given by

$$\lambda = 2 \int_0^{\infty} \frac{\alpha^2(\omega)F(\omega)}{\omega} d\omega, \quad (5)$$

we obtain a value of $\lambda = 1.32$. Tunneling experiments, in contrast, give a higher value of $\lambda = 1.5$. This indicates that we have perhaps underestimated somewhat the strength of the electron-phonon interaction in our work. This could be due to inaccuracies in the Appapillai and Williams⁷ pseudopotential or in the calculations of the Fermi surface and in particular the density of states at the FS. More importantly, we have normalized to 1 the pseudo-wave-functions rather than the real lines. Thus the calculated curve should be multiplied by a constant amount slightly larger than 1, thereby increasing the agreement with tunneling. This will not be done here as we take the attitude that the degree of overall agreement displayed in Fig. 2 is quite satisfactory.

It is of interest before leaving this section, to define a coupling strength $\alpha^2(\omega)$ according to the prescription

$$\alpha^2(\omega) = \alpha^2(\omega)F(\omega)/F(\omega), \quad (6)$$

where $F(\omega)$ is the phonon density of states given by

$$F(\omega) = \int_{\text{FS}} \frac{dS_{\mathbf{k}}}{\hbar v_{\mathbf{k}}} \int_{\text{FS}} \frac{dS_{\mathbf{k}'}}{\hbar v_{\mathbf{k}'}}$$

$$\times \left(\sum_{\lambda} \delta(\omega - \omega_{\lambda}(\mathbf{k}' - \mathbf{k})) \right) / \int_{\text{FS}} \frac{dS_{\mathbf{k}}}{\hbar v_{\mathbf{k}}}. \quad (7)$$

In Eq. (7) the integration over $dS_{\mathbf{k}}$ extends over the Fermi surface and $F(\omega)$ is normalized so that

$$\int_0^{\infty} F(\omega) d\omega = 3 \int \frac{dS_{\mathbf{k}}}{\hbar v_{\mathbf{k}}}. \quad (8)$$

A plot of $\alpha^2(\omega)$ in arbitrary units is given in Fig. 3. We note first of all that it is perfectly well behaved at low frequencies. As previously noted, a one-plane-wave result would give an unphysical diverging result as ω tends towards zero. As ω increases, $\alpha^2(\omega)$ is found to increase roughly linearly. This is in agreement with the data on $\alpha^2(\omega)$ obtained by Rowell, McMillan, and Feldmann.¹⁶ Superimposed on this roughly linear increase in $\alpha^2(\omega)$ with increasing ω are fluctuations, some of which must be due to noise in our computer program. There does, however, appear to be an abrupt increase near 1.6 meV as observed by Rowell *et al.*¹⁶ but there is no evidence of a further abrupt change around 3.1 meV. The abrupt change at 1.6 meV reflects the electronic structure and it is a truly remarkable accomplishment of the tunneling technique that it can be picked up. If we define $F(\omega)$ in a different manner by summing all the phonons in the FBZ, the result for $\alpha^2(\omega)$ is basically the same, including the abrupt increase at 1.6 meV.

IV. ANISOTROPIC ENERGY GAP

We begin with the one-dimensional form of the Eliashberg equations appropriate to the isotropic dirty-limit case. They are a set of two coupled integral equations for a frequency-dependent gap function $\Delta(\omega)$ and a renormalization function $Z(\omega)$, both functions being complex. They are

$$\begin{aligned} \Delta(\omega)Z(\omega) &= \int_0^{\omega_c} d\omega' \text{Re} \left(\frac{\Delta(\omega')}{[\omega'^2 - \Delta^2(\omega')]^{1/2}} \right) \\ &\quad \times [K_+(\omega, \omega') - U_C], \\ [1 - Z(\omega)]\omega &= \int_0^{\omega_c} d\omega' \text{Re} \left(\frac{\omega'}{[\omega'^2 - \Delta^2(\omega')]^{1/2}} \right) \\ &\quad \times K_-(\omega, \omega'), \end{aligned} \quad (9)$$

with

$$\begin{aligned} K_{\pm}(\omega, \omega') &= \int_0^{\infty} dv \alpha^2(v)F(v) \\ &\quad \times \left(\frac{1}{\omega' + \omega + v + i0^+} \frac{1}{\omega' - \omega + v - i0^+} \right). \end{aligned} \quad (10)$$

In Eqs. (9) ω_c is a phonon cutoff taken to be equal to $10 \times \omega_0$ with ω_0 the maximum phonon frequency in Pb and U_C , a Coulomb effective potential which accounts for the Coulomb repulsions between electrons. In what follows we take $U_C = 0.1$.

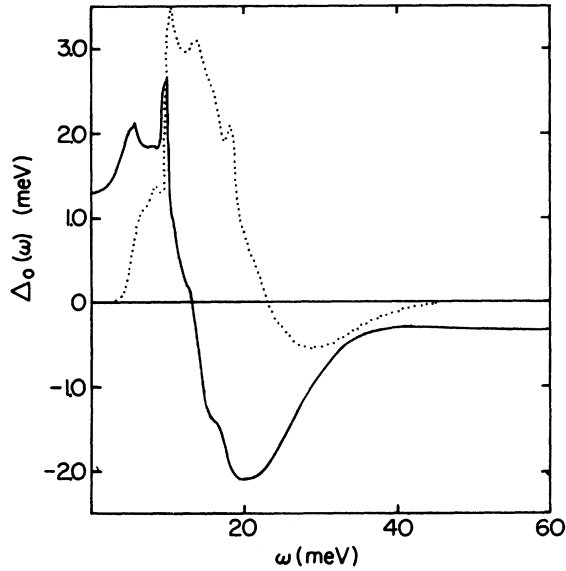


FIG. 4. Real $\Delta_1(\omega)$ (solid curve) and imaginary $\Delta_2(\omega)$ (dotted curve) part of the gap function $\Delta(\omega)$ for the dirty-limit isotropic case.

We have solved the Eliashberg Eqs. (9) with the kernel $\alpha^2(\omega)F(\omega)$ obtained from our four-plane-wave model for the electronic structure and Cowley's model⁸ for the phonons. Results for the real and imaginary parts of $\Delta \equiv \Delta_1 + i\Delta_2$ are shown in Fig. 4 as a function of frequency; they compare

TABLE I. Gap edge $\Delta_0(\theta, \phi)$ and renormalization parameter $\lambda(\theta, \phi)$ for the various points on the Pb Fermi surface where we have made explicit calculations. Intermediate points can be obtained by interpolating between the values given.

θ, ϕ	$\Delta_0(\theta, \phi)$ (meV)	$\lambda(\theta, \phi)$	(θ, ϕ)	$\Delta_0(\theta, \phi)$ (meV)	$\lambda(\theta, \phi)$
1, 1	1.18	1.09	27, 29	1.35	1.31
5, 1	1.12	1.03	45, 31	1.18	1.09
35, 1	1.48	1.55	33, 33	1.45	1.52
45, 1	1.43	1.46	13, 35	1.47	1.62
39, 5	1.46	1.52	23, 35	1.35	1.31
37, 9	1.48	1.57	41, 35	1.12	1.03
45, 9	1.46	1.59	27, 39	1.35	1.31
15, 13	1.48	1.59	45, 39	1.20	1.11
35, 13	1.48	1.57	19, 41	1.39	1.41
33, 19	1.46	1.54	5, 45	1.15	1.07
3, 23	1.15	1.06	13, 45	1.47	1.62
15, 23	1.46	1.57	27, 45	1.36	1.32
23, 23	1.34	1.30	33, 45	1.44	1.52
33, 23	1.43	1.53	39, 45	1.14	1.07
45, 23	1.13	1.04	53, 45	1.24	1.15
19, 29	1.39	1.40			

well with previous results derived from tunneling results on $\alpha^2(\omega)F(\omega)$. These results will form the basis of our calculations of gap anisotropy which require the four-dimensional form of the Eliashberg equations.

Since it is out of the question to iterate to convergence the Eliashberg equations in their four-dimensional form, we will follow here the suggestion of Bennett,⁶ who performs a single iteration based on the dirty-limit results for the gap and renormalization function. Bennett's equations are

$$\Delta(\vec{p}, \omega)Z(\vec{p}, \omega) = \int_0^{\omega_c} d\omega' \operatorname{Re} \left(\frac{\Delta(\omega')}{[\omega'^2 - \Delta^2(\omega')]^{1/2}} \right) \times [K_*(\omega, \omega', \vec{p}) - U_C] \quad (11)$$

and

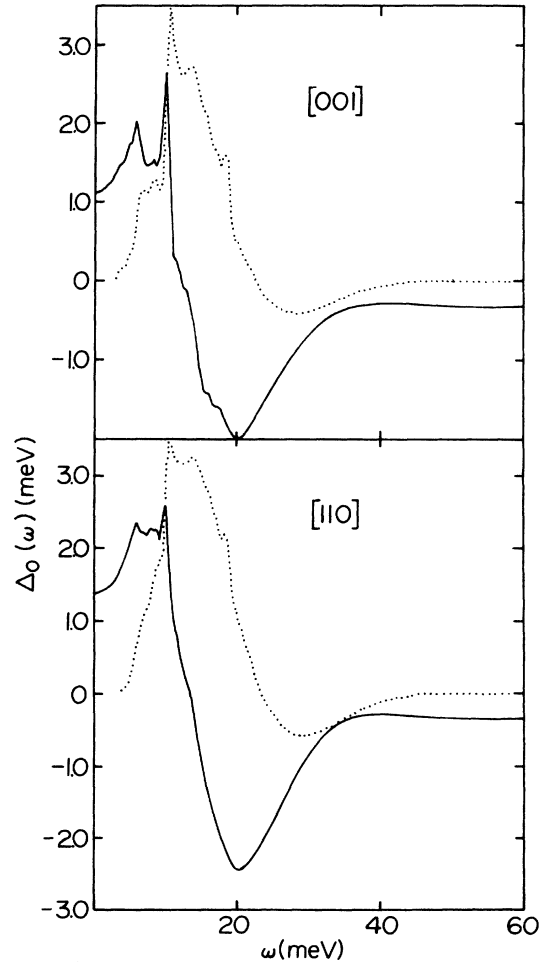


FIG. 5. Real $\Delta_1(\vec{p}, \omega)$ (solid curve) and imaginary $\Delta_2(\vec{p}, \omega)$ (dotted curve) part of the anisotropic gap $\Delta(\vec{p}, \omega)$ for two directions, namely, [001] and [110]. These were obtained by a single iteration of the anisotropic Eliashberg gap equations based on the dirty-limit solutions presented in Fig. 4.

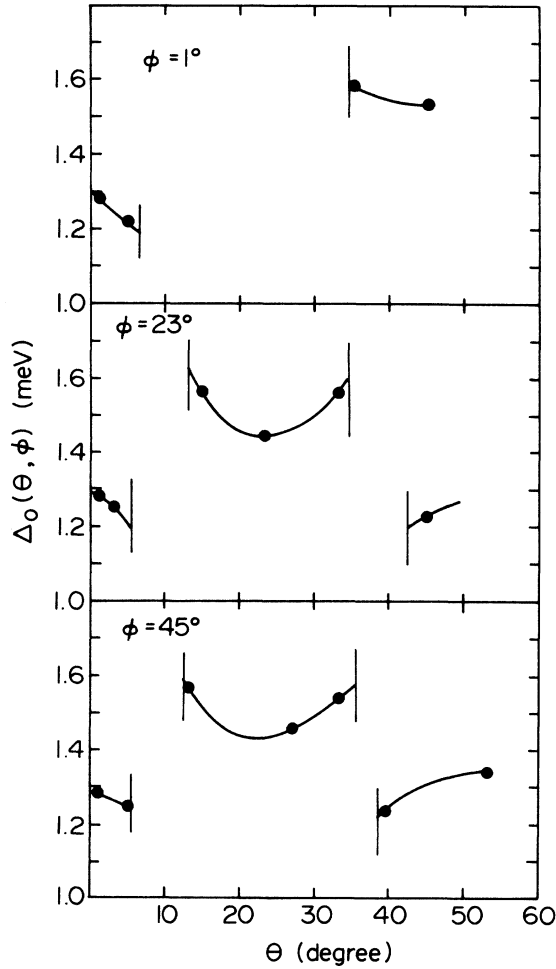


FIG. 6. Gap edge $\Delta_0(\vec{p})$ for three constant ϕ arcs, 1° , 23° , and 45° , as a function of θ . Regions where the Fermi surface of Pb does not exist are indicated by vertical lines. Amount of anisotropy in these curves is considerable. It includes the anisotropy due to the phonon spectrum, the electron-phonon umklapp processes, as well as the electronic structure, i. e., Fermi-surface distortions and multiple-plane-wave effects.

$$[1 - Z(\vec{p}, \omega)]\omega = \int_0^{\omega_c} d\omega' \operatorname{Re} \left(\frac{\omega'}{[\omega'^2 - \Delta^2(\omega')]^{1/2}} \right) \times K_{\pm}(\omega, \omega', \vec{p}),$$

where now

$$K_{\pm}(\omega, \omega', \vec{p}) = \int_0^{\infty} dv \alpha_{\vec{p}}^2(v) F_{\vec{p}}(v) \times \left(\frac{1}{\omega' + \omega + v + i0^*} \frac{1}{\omega' - \omega + v - i0^*} \right). \quad (12)$$

While on the right-hand side of Eqs. (11) we have inserted the dirty-limit values for the gap $\Delta(\omega)$, it is now the directional functions $\alpha_{\vec{p}}^2(v)F_{\vec{p}}(v)$ that ap-

pear. These functions fully contain the anisotropy due to the Fermi surface, the phonon spectrum, and the electron-phonon interaction.

Results for $\Delta(\vec{p}, \omega)$ with \vec{p} on the Fermi surface and pointing in the [001] and the [110] directions are compared in Fig. 5. We see significant variations in these curves and in particular in the gap edge $\Delta_0(\vec{p})$ defined by

$$\Delta_0(\vec{p}) = \operatorname{Re} \Delta(\vec{p}, \omega = \Delta_0(\vec{p})). \quad (13)$$

We have obtained further results for a total of 31 directions.

V. RESULTS AND DISCUSSION

In Fig. 6 we present results for the gap edge in pure single-crystal Pb $\Delta_0(\vec{p})$ for three constant ϕ arcs on the Fermi surface. The angles θ and ϕ are polar angles defined as follows: The polar axis is along [001] and θ is measured from this line. In the plane perpendicular to the polar axis we measure ϕ from the [100] axis. We see in the figure that $\Delta_0(\vec{p})$ exhibits a significant amount of anisotropy. We also see that in some directions large regions are missing, which correspond to (θ, ϕ) regions where there is no Fermi surface. In Table I we record the gaps at those points where it was actually calculated. Also of interest are the anisotropic mass renormalization parameters obtained by inserting the directional $\alpha^2 F_{\vec{p}}(\omega)$ into the right-hand side of Eq. (5). These were calculated and included in Table I.

A good measure of the over-all amount of anisotropy is the mean square anisotropy. We define an anisotropy parameter $a(\vec{p})$ by the equation

$$a(\vec{p}) = [\Delta_0(\vec{p}) - \langle \Delta_0(\vec{p}) \rangle] / \langle \Delta_0(\vec{p}) \rangle, \quad (14)$$

where $\langle f(\vec{p}) \rangle$ is by definition its Fermi-surface average, i. e.,

$$\langle f(\vec{p}) \rangle = \left(\int \frac{dS_{\vec{p}}}{\hbar |\vec{V}(\vec{p})|} f(\vec{p}) \right) / \int \frac{dS_{\vec{p}}}{\hbar |\vec{V}(\vec{p})|}. \quad (15)$$

The mean-square anisotropy a^2 is then by definition

$$a^2 = \langle a^2(\vec{p}) \rangle = \{ \langle \Delta_0^2(\vec{p}) \rangle - [\langle \Delta_0(\vec{p}) \rangle]^2 \} / [\langle \Delta_0(\vec{p}) \rangle]^2. \quad (16)$$

It comes out to be equal to 0.00933, or roughly 0.01, so that $a = \sqrt{a^2} \cong 0.1$, which implies roughly ten percent fluctuations.

It is not possible to compare our results with the experiments of Blackford¹ at the moment because the selection rules he used to assign gaps to various parts of the Fermi surface now appear to be invalid. It is hoped, however, that our calculations will stimulate further experiments. Blackford's results do suggest that the gap is peaked about two values, in agreement with our calculations.

In summary, we have made the first realistic first-principle calculations of gap anisotropy in Pb which include the real phonon spectrum and the distortions of the Fermi surface from sphericity and which also use a four-plane-wave model in the

calculations of the electron-phonon matrix element. At the same time, our calculations yield a value of the isotropic electron-phonon strength function $\alpha^2(\omega)F(\omega)$ which is in good agreement with tunneling results on this quantity.

[†]Research supported by the National Research Council of Canada.

¹B. L. Blackford, *Physica (Utr.)* **55**, 475 (1971).

²C. K. Campbell, R. C. Dynes, and D. G. Walmsley, *Can. J. Phys.* **44**, 2601 (1966).

³C. K. Campbell and D. G. Walmsley, *Can. J. Phys.* **45**, 159 (1967).

⁴G. I. Rochlin, *Phys. Rev.* **153**, 513 (1967).

⁵W. L. McMillan and J. M. Rowell, in *Superconductivity*, edited by R. D. Parks (Dekker, New York, 1969).

⁶A. J. Bennett, *Phys. Rev.* **140**, A1902 (1965).

⁷M. Appapillai and A. R. Williams, *J. Phys. F* **3**, 759 (1973).

⁸E. R. Cowley, *Solid State Commun.* **14**, 587 (1974).

⁹J. R. Anderson and A. V. Gold, *Phys. Rev.* **139**, A1459

(1963).

¹⁰B. N. Brockhouse, T. Arase, G. Caglioti, K. R. Rao, and A. D. B. Woods, *Phys. Rev.* **128**, 1099 (1962).

¹¹R. C. Dynes, J. P. Carbotte, and E. J. Woll, *Solid State Commun.* **6**, 101 (1968).

¹²R. Stedman, L. Almqvist, and G. Nilsson, *Phys. Rev.* **162**, 549 (1967).

¹³R. W. Shaw, Jr., *Phys. Rev.* **174**, 769 (1968).

¹⁴J. P. Carbotte and R. C. Dynes, *Phys. Rev.* **172**, 476 (1968).

¹⁵B. Farnworth and T. Timusk, *Phys. Rev. B* **10**, 2799 (1974).

¹⁶J. M. Rowell, W. L. McMillan, and W. L. Feldmann, *Phys. Rev.* **178**, 897 (1969).